

# Turbulent magnetic Prandtl number and magnetic diffusivity quenching from simulations

T. A. Yousef<sup>1</sup>, A. Brandenburg<sup>2</sup> and G. Rüdiger<sup>3</sup>

<sup>1</sup> Fluid Technology Group, Faculty of Engineering Science and Technology, Norwegian University of Science and Technology, Kolbjørn Hejes vei 2B, N-7491 Trondheim, Norway

<sup>2</sup> NORDITA, Blegdamsvej 17, DK-2100 Copenhagen Ø, Denmark

<sup>3</sup> Astrophysical Institute Potsdam, An der Sternwarte 16, D-14482 Potsdam, Germany

May 22, 2019, Revision: 1.28

**Abstract.** Forced turbulence simulations are used to determine the turbulent kinematic viscosity,  $\nu_t$ , from the decay rate of a large scale velocity field. Likewise, the turbulent magnetic diffusivity,  $\eta_t$ , is determined from the decay of a large scale magnetic field. In the kinematic regime, when the field is weak, the turbulent magnetic Prandtl number,  $\nu_t/\eta_t$ , is about unity. When the field is nonhelical,  $\eta_t$  is quenched when magnetic and kinetic energies become comparable. For helical fields the quenching is stronger and can be described by a dynamical quenching formula.

**Key words.** MHD – Turbulence

## 1. Introduction

The concept of turbulent diffusion is often invoked when modeling large scale flows and magnetic fields in a turbulent medium. Turbulent magnetic diffusion is similar to turbulent thermal diffusion which characterizes the turbulent exchange of patches of warm and cold gas. This concept is also applied to turbulent magnetic diffusion which describes the turbulent exchange of patches of magnetic field with different strengths and direction. Reconnection of magnetic field lines is not explicitly required, but in the long run unavoidable if the magnetic power spectrum is to decrease toward small scales. The idea of Prandtl is that only the energy carrying eddies contribute to the mixing of large scale distributions of velocity and magnetic field structures. This leads to a turbulent magnetic diffusion coefficient  $\eta_t \approx \frac{1}{3}U\ell$ , where  $U$  is the typical velocity and  $\ell$  the scale of the energy carrying eddies. For the kinematic turbulent viscosity one expects similar values. Analytic theory based on the quasilinear approximation also produces similar (but not identical) values of  $\eta_t$  and  $\nu_t$  (e.g. Kitchatinov et al. 1994).

It is usually assumed that the values of  $\eta_t$  and  $\nu_t$  are independent of the molecular (microscopic) viscosity and magnetic diffusivity,  $\nu$  and  $\eta$ . However, in the context of the geodynamo or in laboratory liquid metals the microscopic magnetic Prandtl number,  $P_m = \nu/\eta$  is very small ( $\approx 10^{-5}$ ). This has dramatic consequences for the magnetorotational instability (Balbus & Hawley 1991). This

instability is generally accepted as the main mechanism producing turbulence in accretion discs (Balbus & Hawley 1998). For sufficiently small values of  $P_m$ , however, this instability is suppressed (Rüdiger & Shalybkov 2002). On the other hand, the Reynolds number of the flow is quite large ( $10^5 \dots 10^6$ ) and the flow therefore most certainly turbulent. This led Noguchi et al. (2002) to invoke a turbulent kinematic viscosity,  $\nu_t$ , but to retain the microscopic value of  $\eta$ . The resulting *effective* magnetic Prandtl number they used was  $10^{-2}$  – big enough for the magnetorotational instability to develop. One may wonder, of course, why one should not instead use turbulent values for both coefficients, i.e.  $\nu_t/\eta_t \approx 1$ . This would lead to even more favorable conditions for the magnetorotational instability (Rüdiger et al. 2003).

Similar constraints have also been reported for the convection-driven geodynamo: Christensen et al. (1999) found that there is a minimum value of  $P_m$  of about 0.25 below which dynamo action does not occur at all. Similar results have also been reported by Cattaneo (2003). These results are disturbing, because both for the sun and for the earth,  $P_m \ll 1$ . For  $P_m$  of order unity, on the other hand, earth-like magnetic configurations can more easily be reproduced (see Kutzner & Christensen 2002).

Because of these restrictions, one wonders whether the effective magnetic Prandtl number to be used is not  $P_m$ , but rather the turbulent value,  $P_{m,t} = \nu_t/\eta_t$ . This raises the important questions whether  $P_{m,t}$  is actually of order unity and whether it is independent of the microscopic

value,  $P_m$ . The aim of this paper is to estimate the value of  $P_{m,t}$  using turbulence simulations.

The knowledge of the value of  $P_{m,t}$  is also important for the solar dynamo. The qualitative properties of the dynamo depend on the relative importance of the large scale flows and hence on the magnitude of  $\eta_t$ . If  $\eta_t$  is too large, the influence of a meridional flow of say 10 m/s is small so that only little modification can be expected for the basic  $\alpha\Omega$ -dynamo (Roberts & Stix 1972). In this case, however, we know that conventional dynamo models of the solar activity cycle have difficulty to explain Spörer's law of equatorward sunspot migration. The alternative that the resulting poleward migration can be overcompensated by an internal equatorward flow requires a sufficiently small value of  $\eta_t$ , which implies that  $P_{m,t} > 1$  (Choudhuri et al. 1995; Dikpati & Charbonneau 1999; Bonanno et al 2002).

Given the importance of the value of the turbulent magnetic Prandtl number it is useful to assess the problem using numerical simulations of turbulent flows. We consider weakly compressible nonhelically forced turbulence and use a model similar to that of Brandenburg (2001), but with kinetic helicity fluctuating about zero. Dynamo action for such a model has recently been considered by Haugen et al. (2003). We begin however by first reviewing the basic results for the values of  $\nu_t$  and  $\eta_t$  within the framework of the quasilinear approximation (Rüdiger 1989).

## 2. Results from quasilinear approximation

Denoting the spectral tensor for homogeneous isotropic turbulence by  $\hat{Q}_{ij}(\mathbf{k}, \omega)$ , one finds

$$\nu_t = \frac{4}{15} \iint \frac{\nu^3 k^6 \hat{Q}_{ll}(\mathbf{k}, \omega)}{(\omega^2 + \nu^2 k^4)^2} d\mathbf{k} d\omega \quad (1)$$

for the turbulent viscosity and

$$\eta_t = \frac{1}{3} \iint \frac{\eta k^2 \hat{Q}_{ll}(\mathbf{k}, \omega)}{\omega^2 + \eta^2 k^4} d\mathbf{k} d\omega \quad (2)$$

for the turbulent magnetic diffusivity (see Rüdiger 1989). Obviously, both quantities are of the same order of magnitude, but they are not identical. In the limits  $\nu, \eta \rightarrow 0$  the expressions are drastically simplified, i.e.

$$\nu_t = \frac{1}{15} \int_{-\infty}^{\infty} \langle \mathbf{u}'(\mathbf{x}, t) \mathbf{u}'(\mathbf{x}, t + \tau) \rangle d\tau \quad (3)$$

and

$$\eta_t = \frac{1}{6} \int_{-\infty}^{\infty} \langle \mathbf{u}'(\mathbf{x}, t) \mathbf{u}'(\mathbf{x}, t + \tau) \rangle d\tau, \quad (4)$$

so that for the turbulent magnetic Prandtl number

$$P_{m,t} = \frac{\nu_t}{\eta_t} = \frac{2}{5} \quad (5)$$

results, in good agreement to the results of Nakano et al. (1979).

In the remainder of this paper we estimate  $\nu_t$  and  $\eta_t$  numerically by considering the decay of an initial large scale velocity or magnetic field, respectively, in the presence of small scale turbulence.

## 3. The model

The equations describing compressible isothermal hydro-magnetic flows with constant sound speed,  $c_s$ , are

$$\frac{D\mathbf{u}}{Dt} = -c_s^2 \nabla \ln \rho + \frac{\mathbf{J} \times \mathbf{B}}{\rho} + \mathbf{F}_{\text{visc}} + \mathbf{f}, \quad (6)$$

$$\frac{D \ln \rho}{Dt} = -\nabla \cdot \mathbf{u}, \quad (7)$$

$$\frac{\partial \mathbf{B}}{\partial t} = \nabla \times (\mathbf{u} \times \mathbf{B}) + \eta \nabla^2 \mathbf{B}, \quad (8)$$

where  $\mathbf{u}$  is the velocity,  $\rho$  the density,  $\mathbf{B}$  is the magnetic field, and  $\mathbf{J} = \nabla \times \mathbf{B}/\mu_0$  is the current density with  $\mu_0$  being the vacuum permeability. The viscous force is

$$\mathbf{F}_{\text{visc}} = \nu (\nabla^2 \mathbf{u} + \frac{1}{3} \nabla \nabla \cdot \mathbf{u} + 2\mathbf{S} \cdot \nabla \ln \rho), \quad (9)$$

where  $\mathbf{S}_{ij} = \frac{1}{2}(u_{i,j} + u_{j,i}) - \frac{1}{3}\delta_{ij}\nabla \cdot \mathbf{u}$  is the traceless rate of strain tensor.

We focus on the case where the forcing,  $\mathbf{f}$ , occurs at a wavenumber around  $k_f = 10$ . The forcing is such that the turbulence is subsonic and nonhelical. We consider two different periodic initial conditions,

$$\mathbf{B} = (\cos k_1 z, 0, 0) B_0 \quad (\text{nonhelical}) \quad (10)$$

and

$$\mathbf{B} = (\cos k_1 z, \sin k_1 z, 0) B_0 \quad (\text{helical}), \quad (11)$$

where  $B_0$  is the amplitude of the initial field. In the fully helical case one may expect a different decay time because the magnetic helicity is a conserved quantity in the limit of small magnetic diffusivity. For the velocity field we use similar initial conditions, but we do not expect this to be sensitive to helicity, because kinetic helicity is not conserved in the limit  $\nu \rightarrow 0$ , and would only be conserved in the unphysical case  $\nu = 0$ .

## 4. Results

### 4.1. Decay of $\bar{u}$ and $\bar{\mathbf{B}}$

We begin by considering the decay of a helical large scale magnetic field and compare it with the decay of a large scale helical velocity field in a purely hydrodynamic simulation; see Fig. 1. Here, large scale velocity and magnetic fields are defined as horizontal averages over  $x$  and  $y$ ; the result is denoted by  $\bar{u}$  and  $\bar{\mathbf{B}}$ , respectively. The magnetic field decay is initially slow and then speeds up, while the decay of the velocity field is immediately fast. This suggests that the turbulent magnetic diffusivity is affected by the strong initial field that in turn gives rise to a quenching of the turbulent magnetic diffusivity. Strong means

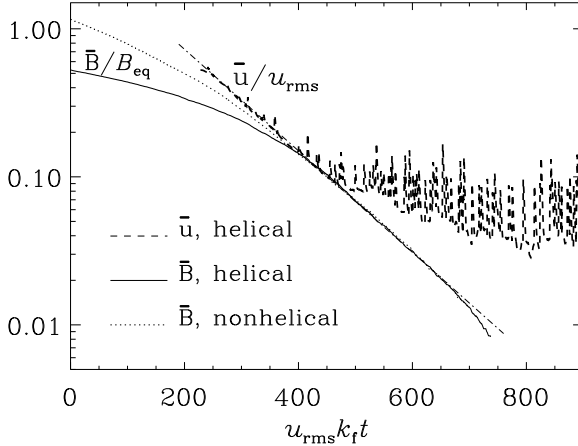


**Fig. 1.** Decay of large scale helical velocity and magnetic fields (dashed and solid lines, respectively). The graph of  $\bar{u}(t)$  has been shifted so that both  $\bar{u}(t)$  and  $\bar{B}(t)$  share the same tangent (dash-dotted line), whose slope corresponds to  $\nu_t = \eta_t = 0.86 u_{\text{rms}} / k_f$ . The decay of a nonhelical magnetic field is shown for comparison (dotted line).

that the magnetic field strength is comparable with the equipartition field strength,  $B_{\text{eq}} = \langle \mu_0 \rho \mathbf{u}^2 \rangle^{1/2}$ . The initially strong large scale flow and the associated vorticity, on the other hand, do not and are also not expected to affect the turbulent viscosity and the associated decay of this large scale flow. For  $|\bar{\mathbf{B}}| \ll B_{\text{eq}}$ , however, both  $\bar{u}$  and  $\bar{B}$  decay at the same rates,  $\lambda_u$  and  $\lambda_B$ , respectively. This allows us to calculate

$$\nu_t = \lambda_u / k_1^2, \quad \eta_t = \lambda_B / k_1^2, \quad (12)$$

where  $k_1$  is the wavenumber of the initial large scale velocity and magnetic fields. From the present simulations, where  $k_f / k_1 = 10$ , we find

$$\nu_t \approx \eta_t = (0.8 \dots 0.9) \times u_{\text{rms}} / k_f \quad (\text{for } \bar{\mathbf{B}}^2 \ll B_{\text{eq}}^2). \quad (13)$$

Once  $|\bar{u}|$  has decreased below a certain level ( $< 0.1 u_{\text{rms}}$ ), it cannot decay further and continues to fluctuate around  $0.08 u_{\text{rms}}$ , corresponding to the level of the rms velocity of the turbulence at  $k = k_1$  (see the dashed line in Fig. 1).

The quenching of the magnetic diffusivity,  $\eta_t = \eta_t(\bar{\mathbf{B}})$ , can be obtained from one and the same run by simply determining the decay rate,  $\lambda_B(\bar{B}) = d \ln \bar{B} / dt$ , at different times, corresponding to different values of  $\bar{B} = |\bar{\mathbf{B}}|$ ; see Fig. 2. To describe departures from purely exponential decay we adopt a  $\bar{\mathbf{B}}$ -dependent  $\eta_t$  expression of the form

$$\eta_t(\bar{\mathbf{B}}) = \eta_{t0} / (1 + a \bar{\mathbf{B}}^2 / B_{\text{eq}}^2), \quad (14)$$

where  $\eta_{t0}$  is the unquenched (kinematic) value of  $\eta_t$ , described approximately by Eq. (13), and  $a$  is a fit parameter. According to Cattaneo & Vainshtein (1991) the parameter  $a$  is expected to be of the order of the magnetic Reynolds number based on the microscopic magnetic diffusivity,

$$R_m = u_{\text{rms}} k_f / \eta. \quad (15)$$

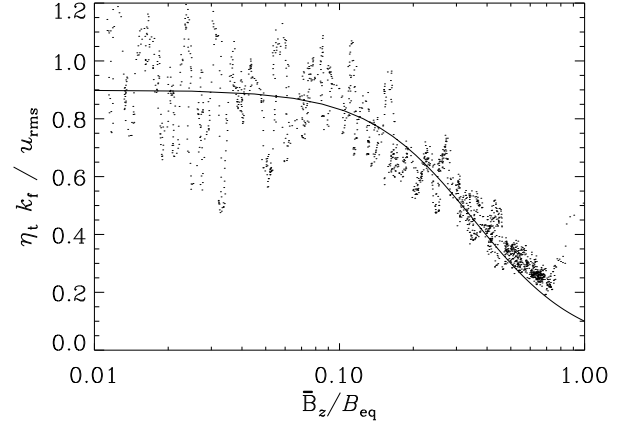


**Fig. 2.** Dependence of the turbulent diffusion coefficient on the magnitude of the mean field. The initial field is helical.  $R_m \approx 20$ . The data are best fitted by  $a = 8 = 0.4 R_m$ .

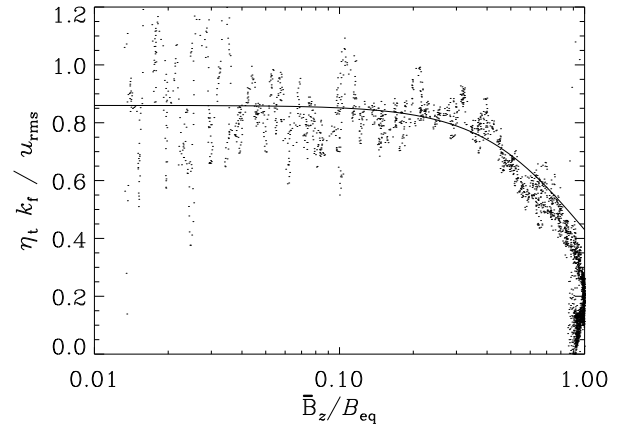


**Fig. 3.** Dependence of the turbulent diffusion coefficient on the magnitude of the mean field. The initial field is nonhelical.  $R_m \approx 20$ . The data are best fitted by  $a = 1$ , independent of  $R_m$ .

Figure 2 suggests that  $a \approx 0.4 R_m$ .

Before we discuss the effective quenching behavior of  $\eta_t$  in more detail we should note that Eq. (14), and in particular the value of  $a$ , do not apply universally and depend on the field geometry. This is easily demonstrated by considering a nonhelical initial field. In that case the decay becomes unquenched already for  $\bar{\mathbf{B}}^2 / B_{\text{eq}}^2 \approx 1$ . Equation (14) can still be used as a reasonable fit formula, but now  $a = 1$  produces a good fit (independent of  $R_m$ ); see Fig. 3.

In the nonhelical case there is an initial phase where the field increases due to the wind-up of the large scale field. Since we measure  $\eta_t$  from the decay rate of the large scale field, this would formally imply negative values of  $\eta_t$ . Traces of this effect can still be seen in Fig. 3 near  $\bar{\mathbf{B}}^2 / B_{\text{eq}}^2 = 1$ . For this reason our method can only give reliable results if  $|\bar{\mathbf{B}}| \lesssim 0.8 B_{\text{eq}}$ . In the case of a helical initial field, on the other hand, we have  $\bar{\mathbf{J}} \times \bar{\mathbf{B}} = 0$ , i.e.

the large scale field is force-free and interacts only weakly with the turbulence. In particular, there is no significant amplification from the initial wind-up of the large scale field.

#### 4.2. Comparison with the dynamical quenching model

In the case of a helical field and for  $\bar{\mathbf{B}}^2/B_{\text{eq}}^2 \gtrsim R_m^{-1}$  the slow decay of  $\bar{\mathbf{B}}$  is related to the conservation of magnetic helicity. As discussed already by Blackman & Brandenburg (2002), this behavior is related to the phenomenon of selective decay (e.g. Montgomery et al. 1978) and can be described by the dynamical quenching model. This model goes back to an early paper by Kleerorin & Ruzmaikin (1982), but it applies even to the case where the turbulence is nonhelical and where there is no  $\alpha$  effect in the usual sense. However, the magnetic contribution to  $\alpha$  is still non-vanishing because it is driven by the helicity of the large scale field.

To demonstrate this quantitatively we solve, in the one mode approximation ( $\mathbf{k} = \mathbf{k}_1$ ) with  $\bar{\mathbf{B}} = \hat{\mathbf{B}} \exp(i\mathbf{k}_1 z)$ , the mean-field induction equation

$$\frac{d\hat{\mathbf{B}}}{dt} = i\mathbf{k}_1 \times \hat{\mathcal{E}} - \eta k_1^2 \hat{\mathbf{B}} \quad (16)$$

together with the dynamical  $\alpha$ -quenching formula [Eq. (13) of Blackman & Brandenburg (2002)]

$$\frac{d\alpha}{dt} = -2\eta k_f^2 \left( \alpha + \tilde{R}_m \frac{\text{Re}(\hat{\mathcal{E}}^* \cdot \hat{\mathbf{B}})}{B_{\text{eq}}^2} \right), \quad (17)$$

where

$$\hat{\mathcal{E}} = \alpha \hat{\mathbf{B}} - \eta_t i \mathbf{k}_1 \times \hat{\mathbf{B}} \quad (18)$$

is the electromotive force, and  $\tilde{R}_m$  is defined as the ratio  $\eta_{t0}/\eta$ , which is expected to be close to the value of  $R_m$  as defined by Eq. (15).

In Fig. 4 we show the evolution of  $\bar{\mathbf{B}}/B_{\text{eq}}$  for helical and nonhelical initial conditions,  $\hat{\mathbf{B}} \propto (1, i, 0)$  and  $\hat{\mathbf{B}} \propto (1, 0, 0)$ , respectively. In the case of a nonhelical field, the decay rate is not quenched at all, but in the helical case quenching sets in for  $\bar{\mathbf{B}}^2/B_{\text{eq}}^2 \gtrsim R_m^{-1}$ .

In the helical case, the onset of quenching at  $\bar{\mathbf{B}}^2/B_{\text{eq}}^2 \approx R_m^{-1}$  is well reproduced by the simulations. In the nonhelical case, however, some weaker form of quenching sets in when  $\bar{\mathbf{B}}^2/B_{\text{eq}}^2 \approx 1$  (Fig. 3). We refer to this as standard quenching (e.g. Kitchatinov et al. 1994) which is known to be always present. In Blackman & Brandenburg (2002) this was modeled by allowing in Eq. (18)  $\eta_t$  to be  $\bar{\mathbf{B}}$ -dependent. They adopted the formula

$$\eta_t = \eta_{t0}/(1 + \tilde{g}|\langle \bar{\mathbf{B}} \rangle|/B_{\text{eq}}) \quad (19)$$

and found that, for a range of different values of  $R_m$ ,  $\tilde{g} = 3$  resulted in a good description of the simulations of cyclic  $\alpha\Omega$ -type dynamos (Brandenburg et al. 2002). We emphasize that this  $\eta_t$  is *not* used in a diagnostic way as in

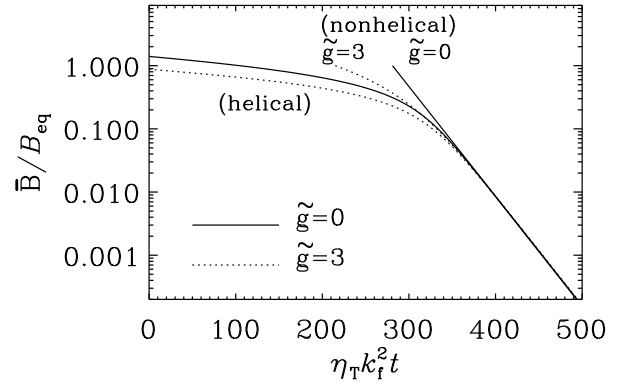


**Fig. 4.** Dynamical quenching model with helical and nonhelical initial fields. The quenching parameters are  $\tilde{g} = 0$  (solid line) and 3 (dotted line). The graph for the nonhelical cases has been shifted in  $t$  so that one sees that the decay rates are asymptotically equal at late times.

Eq. (14), but rather in the numerical solution of Eqs (16) and (17). The resulting decay law, shown as a dotted line in Fig. 4, agrees now with the decay law seen in the turbulence simulations (Fig. 1). The helical case with  $\tilde{g} = 3$  is still compatible with the simulations.

#### 5. Independence of microscopic viscosity

Finally we need to show that the turbulent magnetic Prandtl number is indeed independent of the microscopic magnetic Prandtl number. In Fig. 5 we plot the decay rates, obtained by differentiating  $\ln \bar{\mathbf{B}}(t)$ , for three different values of the microscopic viscosity, keeping  $\eta$  fixed. The resulting values of the flow Reynolds number,  $\text{Re} = u_{\text{rms}} k_f / \nu$ , vary between 20 and 150, giving  $P_m$  in the range between 0.1 and 1. Within plot accuracy the three values of  $\lambda_B$  turn out to be identical.

The numerical resolution used in most of the models is  $128^3$  mesh points. However, as  $\text{Re}$  is increased, higher resolution is required. For  $\text{Re}=80$  we used  $256^3$  mesh points and for  $\text{Re}=150$  we used  $512^3$  mesh points. This implies a Reynolds number,  $u_{\text{rms}} \Delta x / \nu$ , based on the mesh spacing  $\Delta x$ , of about 18. Empirically we know that larger values are not generally possible.

#### 6. Conclusions

The turbulence simulations presented here have shown that the turbulent magnetic Prandtl number is always of order unity, regardless of the values of the *microscopic* magnetic Prandtl number. The value of  $2/5$ , obtained from the quasilinear approximation, cannot be confirmed. This might be because the idealizing assumption made in order to apply the quasilinear approximation are not justified. Our results have also shown that, for nonhelical magnetic fields, the turbulent magnetic diffusivity is quenched when the magnetic energy becomes comparable to the kinetic

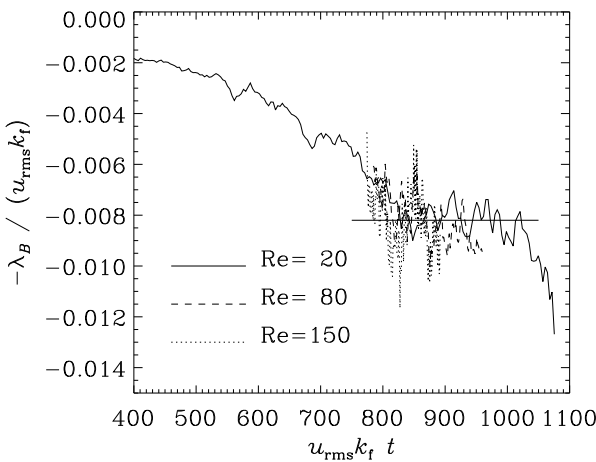


**Fig. 5.** Decay rate for three different values of  $Re$  and  $R_m = 20$  (fixed), corresponding to values of  $P_m = R_m/Re$  ranging from 0.1 to 1. All three curves have a plateau where the value of  $\lambda_B$  is the same.

energy. For helical magnetic fields, however, an apparent suppression of the decay rate is observed which agrees with predictions from a dynamical quenching model. If this suppression is described by an algebraic expression, quenching would set in for magnetic energies much below the kinetic energy.

The present work demonstrates that the dynamical quenching approach is not restricted to dynamos, but it can also deal with decay problems, as was already mentioned in Blackman & Brandenburg (2002). The dynamical quenching model is usually formulated in terms of  $\alpha$ , but for helical mean fields  $\bar{\mathbf{J}}$  and  $\bar{\mathbf{B}}$  are parallel and the separation into contributions from  $\alpha\bar{\mathbf{B}}$  and  $\eta_t\bar{\mathbf{J}}$  becomes less meaningful. It is for this reasons that an  $\alpha$  term appears in the description of the decay of helical fields, rather than a dynamical contribution to  $\eta_t$ -quenching.

The remaining quenching of  $\eta_t$  that affects both helical and nonhelical fields is consistent with an algebraic quenching formula that is non-catastrophic, i.e. independent of the microscopic magnetic diffusivity.

*Acknowledgements.* Use of the supercomputers in Odense (Horseshoe), Trondheim (Gridur), and Leicester (Ukaff) is acknowledged.

## References

Balbus, S. A., & Hawley, J. F. 1991, *ApJ*, 376, 214  
 Balbus, S. A., & Hawley, J. F. 1998, *Rev. Mod. Phys.*, 70, 1  
 Blackman, E. G., & Brandenburg, A. 2002, *ApJ*, 579, 359  
 Bonanno, A., Elstner, D., Rüdiger, G., & Belvedere, G. 2002, *A&A*, 390, 673  
 Brandenburg, A. 2001, *ApJ*, 550, 824  
 Brandenburg, A., Dobler, W., & Subramanian, K. 2002, *Astron. Nachr.*, 323, 99 (astro-ph/0111567)  
 Cattaneo, F. 2002, in *Modelling of Stellar Atmospheres*, ed. N. E. Piskunov, W. W. Weiss, & D. F. Gray (Astron. Soc. Pac. Conf. Ser.), (in press)

Cattaneo, F., & Vainshtein, S. I. 1991, *ApJ*, 376, L21  
 Choudhuri, A.R., Schüssler, M., & Dikpati, M. 1995, *A&A*, 303, L29  
 Christensen, U., Olson, P., & Glatzmaier, G. A. 1999, *Geophys. J. Int.*, 138, 393  
 Dikpati, M., & Charbonneau, P. 1999, *ApJ*, 518, 508  
 Haugen, N. E., Brandenburg, A., & Dobler, W. 2003, *Kitchatinov, L. L., Rüdiger, G., & Pipin, V. V. 1994, *Astron. Nachr.*, 315, 157*  
 Kleeorin, N. I., & Ruzmaikin, A. A. 1982, *Magnetohydrodynamics*, 18, 116  
 Kleeorin, N. I., Rogachevskii, I., & Ruzmaikin, A. 1995, *A&A*, 297, 159  
 Kutzner, C., & Christensen, U. R. 2002, *Phys. Earth Planet Int.*, 131, 29  
 Montgomery, D., Turner, L., & Vahala, G. 1978, *Phys. Fluids*, 21, 757  
 Nakano, T., Fukushima, T., Unno, W., & Kondo, M. 1979, *PASJ*, 31, 713  
 Noguchi, K., Pariev, V. I., Colgate, S. A., Beckley, H. F., & Nordhaus, J. 2002, *ApJ*, 575, 1151  
 Roberts, P., & Stix, M. 1972, *A&A*, 18, 453  
 Rüdiger, G. 1989, *Differential rotation and stellar convection: Sun and solar-type stars*. (Gordon & Breach Science Publishers: New York)  
 Rüdiger, G., & Shalybkov, D. 2002, *Phys. Rev. E*, 66, 016307  
 Rüdiger, G., Schultz, M., & Shalybkov, D. 2002, *astro-ph/0212063*